Original Article
MiR-29a-3p down-regulation of MMP-2 expression affects proliferation and apoptosis of smooth muscle cells in rats with abdominal aortic aneurysm

Xuhua Tang[1*], Jianju Feng[2*], Hongming Qi[1], Diping Luo[3], Hui Zhang[1], Cansong Zhao[1], Yinhai Ni[1], Chendong Yuan[1]

Departments of [1]General Surgery, [2]Radiology, [3]Gastrointestinal Surgery, Zhuji Hospital Affiliated to Shaoxing University, Shaoxing, Zhejiang, China. *Equal contributors.

Abstract: Objective: To find out the impact of miR-29a-3p on the regulation of MMP-2 expression, and the proliferation and apoptosis of smooth muscle cells in rats with abdominal aortic aneurysm. Methods: A rat model of abdominal aortic aneurysm was established for harvesting primary smooth muscle cells, which were then transfected with miR-29a-3p analog, MMP-2 interference, or both. The targeted relationship between miR-29a-3p and MMP-2 was verified with the use of dual-luciferase reporter assay. The expression, proliferation, cycle, and apoptosis of miR-29a-3p, PCNA, MMP-2, N-cadherin, Bax, and Bcl-2 were determined by qRT-PCR, Western blot, MTT assay, and flow cytometry, respectively. Results: MiR-29a-3p negatively regulated MMP-2. Compared with the Normal group, the other groups had declined levels of miR-29a-3p, PCNA, N-cadherin and Bcl-2, elevated expressions of MMP-2 and Bax, retarded proliferation rate, elevated apoptosis rate, and arrested cell cycle (all P<0.05). Compared with the Model group, the miR-29a-3p mimic group and si-MMP-2 group had elevated expressions of PCNA, N-cadherin, and Bcl-2, reduced expression of MMP-2 and Bax, aggravated proliferation rate, reduced apoptosis rate, and shortened cell cycle (all P<0.05). Compared with the miR-29a-3p mimic group, the miR-29a-3p mimic + oe-MMP-2 group had reduced mRNA and protein levels of PCNA, N-cadherin and Bcl-2, elevated mRNA and protein levels of Bax, retarded proliferation rate, elevated apoptosis rate, and prolonged cell cycle (all P<0.05). Conclusion: MiR-29a-3p can down-regulate the expression of MMP-2, as well as facilitate proliferation, and inhibit apoptosis of smooth muscle cells in rats with abdominal aortic aneurysm.

Keywords: miR-29a-3p, MMP-2, abdominal aortic aneurysm, smooth muscle cells

Introduction

Abdominal aortic aneurysm (AAA) is a common disease [1]. Clinical data from different populations show that its prevalence in males is from 2.4% to 16.9%, and in females over 65 years is from 0.5% to 2.2% [2]. In patients with AAA, 60% died from other cardiovascular causes, such as myocardial infarction, or stroke [3]. AAA is associated with aortic dilation diameter ≥5 mm, that occurs below the renal artery, and is caused by extensive vascular inflammation and maladaptive remodeling of the aortic wall [4, 5]. Although various clinical and laboratory studies have given insight into the pathogenesis of AAA, the underlying mechanisms remain to be elucidated [6]. Increasing evidence has shown that vascular smooth muscle cells

(VSMCs) are involved in the development of AAA [7-9]. VSMCs provide a source of elastin, which is of great importance in maintaining the elasticity of the aortic wall [10]. However, during the development of AAA, proteolysis induces the degradation of the dielectric layer, leading to a decline in elastin content and an expansion of the aortic wall, which results in an aggravation of AAA. The lack of elastin is followed by a compensatory increase in collagen synthesis, which contributes to the remodeling of aortic walls and improving of AAA [11]. The decline in elastin is attributed to the senescence and apoptosis of VSMCs [12].

miRNAs are a small class of non-coding RNAs that have been proven to act as target tumor suppressor genes that inhibit the proliferation

and migration of smooth muscle cells, and also affecting angiogenesis [13-16]. Most reports on miR-29a-3p are related to tumors where miR-29a-3p can inhibit various tumors, such as laryngeal cancer, liver cancer and thyroid cancer [17-19]. However, there is no report showing the relationship between miR-29a-3p and AAA. Matrix metalloproteinases (MMPs) are essential for physiological processes; for instance, homeostasis, wound healing, as well as tissue remodeling and resorption [20]. Patients with AAA exhibit higher plasma MMP-9 levels, and they have more MMP-9 mRNA in their aortic tissues than in typical aortic tissues [21]. Besides, MMP-2 and MMP-9 have an impact on the occurrence of aneurysms, and there is a promotion and dependence relationship between MMP-2 and MMP-9 proteases during the occurrence of AAA [22].

Bioinformatic prediction found a targeted relationship between miR-29a-3p and MMP-2. Therefore, we speculated that miR-29a-3p may inhibit proliferation and facilitate the apoptosis of smooth muscle cells by targeting the down-regulation of MMP-2 expression, and then aggravating AAA.

Methods

Animals

In this experimental study, adult Wistar rats, weighing 200-225 g, housed at room temperature with free access to food, were used for the establishment of AAA models by giving them intracavitary elastase and extracavitary $CaCl_2$. At first, the rats were anesthetized with isoflurane, and 10 mm of the infrarenal aortaventralis was exposed by midline laparotomy. Thereafter, 30 U of porcine pancreatic elastase (135 U/mg; Elastin Products Company, Owensville, MO) was injected into aorta *via* an SP10 polyethylene catheter (Natsume Seisakusho, Tokyo, Japan) which was already guided and inserted into the right common femoral artery. The aorta was wrapped in gauze that was immersed in 0.5 mol/l $CaCl_2$ (Sigma-Aldrich, Tokyo, Japan) for 20 min; meanwhile, elastase was added. After 7 days, the rats were euthanized for later experiments through cervical dislocation after anesthesia, which was performed *via* intraperitoneal injection with 3% sodium pentobarbital solution (300 mg/Kg). All procedures involving animals were done in accordance with the ethical standards of Zhuji Hospital Affiliated to Shaoxing University, where the experiments were performed.

Isolation, culture and transfection of smooth muscle cells

The normal and modeled rats were sacrificed and collected for their medial membrane of aortic tissue in a sterile environment. Next, the blood vessels and adipose tissues were removed, and the blood vessels were treated with trypsin for 30 min at 37°C, and removed for the outer membrane. After cutting and centrifugation, the supernatant was discarded. The samples were added with RPMI-1640 (Gibco, USA) containing 10% fetal bovine serum (Gibco, USA) for cell resuspension. The cells were adherently cultured to 90% density, trypsinized, placed into six-well plates in a 50 ml/l CO_2 incubator at 37°C. The cells were observed to be epithelioid-like and spread in a sheet-like manner under an inverted microscope.

Smooth muscle cells grown in log phase were seeded in 6-well culture plates at a density of $1*10^5$/well, and RPMI-1640 medium (Gibco, USA) containing no serum and double antibody was used one day before transfection. There smooth muscle cells of rats were divided into 7 groups: Normal group (smooth muscle cells from normal rats), Model group (untreated smooth muscle cells from model rats), NC mimic group (cells from model rats transfected with NC mimic), miR-29a-3p mimic group (cells from model rats transfected with miR-29a-3p mimic), si-NC group, si-MMP-2 group (cells from model rats transfected with si-MMP-2), miR-29a-3p mimic + oe-MMP-2 group (cells from model rats transfected with miR-29a-3p mimic + oe-MMP-2). The sequence powder was from Jima, Suzhou, China. The cells were transfected for 6 h according to the instructions of Lipofectamine 2000, and then the medium was replaced by RPMI-1640 containing 10% fetal bovine serum (Gibco, USA). After another 48 h, the cells were harvested for subsequent experiments.

Dual-luciferase reporter assay

The binding sites of miR-29a-3p and MMP-2 were analyzed *via* the biological prediction website (www.targetscan.org). Then, the targeting relationship between miR-29a-3p and MMP-2

Table 1. Primer sequence of qRT-PCR

Name	Sequence
MiR-29a-3p	F: 5'-TAACCGATTTCAAATGGTGCTA-3'
	R: 5'-AGCAGGTCCGAGGTATTC-3'
MMP-2	F: 5'-GATTGATGCCGTGTACGAGG-3'
	R: 5'-AGTCTGCGATGAGCTTCGG-3'
PCNA	F: 5'-TTTGAGGCACGCCTGATCC-3'
	R: 5'-GGAGACGTGAGACGAGTCCAT-3'
N-cadherin	F: 5'-GCTGGCCGACATGTATGGTG-3'
	R: 5'GGTGAAACTGTTCATACGTGTCCAA-3'
Bcl-2	F: 5'-ATGCCTTTGTGGAACTATATGGC-3'
	R: 5'-GGTATGCACCCAGAGTGATGC-3'
Bax	F: 5'-TGAAGACAGGGGCCTTTTTG-3'
	R: 5'-AATTCGCCGGAGACACTCG-3'
U6	F: 5'-GCTCCCTTCGGCAGCACA-3'
	R: 5'-GAGCTATTCGCACCAGAGGA-3'
GAPDH	F: 5'-GGTGCCGAGTACGTGGTGC-3'
	R: 5'-CCCAGCATCGAAGGTAGAGGT-3'

was then verified by a dual-luciferase assay. The target gene MMP-2 dual-luciferase reporter vector, PGL3-MMP-2wt, and the mutants that bound to the miR-29a-3p binding site, PGL3-MMP-2mut, were constructed, respectively. The Rellina plasmid and the two reporter vectors were co-transfected into HEK293T cells with the miR-29a-3p plasmid and the NC plasmid, respectively. After 24 h of cell transfection, dual-luciferase assays were performed. The cells of each group were lysed, centrifuged at 12,000 rpm for 1 min, and collected for supernatant. The kits were purchased from Promega, USA, and the detection for luciferase activity was done strictly according to the kit instruction, and as follows. The lysed cell samples were added into the EP tubes. Every 10 µl of the sample was mixed with 100 µl of the firefly luciferase working solution to detect the firefly luciferase activity, and then 100 µl of the Renilla luciferase working solution was added for the detection of Renilla luciferase activity. Relative luciferase activity = firefly luciferase activity/renilla luciferase activity [23].

qRT-PCR

The cells in each group were collected after 48 h of transfection. Total RNA was extracted by Trizol (16096020, Thermo Fisher Scientific, New York, USA; B1802, Harbin Haigene, China). The cDNA was synthesized by TaqMan MicroRNA Assays Reverse Transcription Primer (Thermo scientific, USA). Quantitative PCR detection was performed by SYBR® PremixExTaq™ II Kit (Xingzhi, China). The following components were added in sequence: 25 µl of SYBR® PremixExTaq™ II (2×), 2 µl of PCR forward and reverse primers, 1 µl of ROXReferenceDye (50×), 4 µl of DNA template, and 16 µl of ddH$_2$O. Fluorescence quantitative PCR was performed with AB¹PRISM® 7300 (Shanghai Kunke, China). The reaction conditions were as follows, 10 min of pre-denaturation at 95°C, followed by 32 cycles of 95°C for 15 s and 60°C for 30 s, and another 72°C for 1 min. $\Delta Ct = CT_{(target\ gene)} - CT_{(GAPDH)}$, $\Delta\Delta Ct = \Delta Ct_{(experimental\ group)} - \Delta Ct_{(control\ group)}$. U6 was an internal reference for miR-29a-3p, and GAPDH for the others. The $2^{-\Delta\Delta Ct}$ indicated the relative expression of each target gene. Primers are shown in **Table 1**.

Western blot

After 48 h of cell transfection and culture, the cells were washed 3 times with pre-cooled PBS and extracted for total protein using RIPA lysate containing PMSF (R0010, Solarbio, Beijing, China). BCA kit (Thermo, USA) was used to measure protein concentration, and deionized water was used for zero set. The sample was mixed with loading buffer, boiled in a metal bath at 100°C for 10 min, and mixed with 50 µg protein sample, followed by electrophoresis for 3 h at a constant voltage of 70 V. The protein was then transferred to PVDF membrane (ISEQ00010, Millipore, Billerica, MA, USA) at a constant flow of 150 mA, and sealed in 5% skimmed milk at 4°C for 2 h. After that, the protein was washed with TBST, incubated with primary antibodies anti-rabbit anti-mouse MMP-2 (ab215986, 1:5,000, Abcam, UK), PCNA (ab29, 1 µg/ml, Abcam, UK), N-cadherin (ab18203, 1 µg/ml, Abcam, UK), Bax (ab32503, 1:1,000, Abcam, UK), Bcl-2 (ab182858, 1:1,000, Abcam, UK), GAPDH (ab22555, 1:2,000, Abcam, UK) overnight at 4°C, then washed 3 times with TBST, 6 min each time. Thereafter, the protein was incubated with HRP labeled goat anti-rabbit IgG antibody (1:5,000, Beijing Zhongshan, China) for 2 h, washed 3 times with TBST, 6 min for each time, and then immersed in TBS. Equal volume of liquid A and liquid B from ECL fluorescence detection kit (NB-3501, Ameshame, UK) were evenly mixed, and 200 µl of which was dropped onto the membrane for exposure and imaging in a gel imager. The image analysis sys-

tem (bio-rad, USA) was applied for photographs, and the Image J software was used for analyses.

MTT

The cells were conventional digested, collected, counted, and seeded in a 96-well plate with $3\text{-}6*10^3$ cells per well and a volume of 100 µl per well (6 duplicated wells). Then, 20 µl of MTT solution (Gibco, USA) at a concentration of 5 mg/ml was added in each well at 24 h, 48 h, and 72 h. After another 4 h of incubation in the dark, 100 µl of DMSO was added to each well, and the optical density of each well was read with an enzyme-linked immunosorbent detector (NYW-96M, Beijing Noah, China) at 495 nm. The cell viability curve was plotted with the time point as the abscissa and the optical density as the ordinate.

Flow cytometry

Cells were washed 3 times with PBS and centrifuged at 2,000 r/min for 20 min, then, the supernatant was discarded, and the cell concentration was adjusted to about $1*10^5$/ml with PBS. After that, the sample was added with 1 ml of pre-cooled 75% ethanol, placed in 4°C for 1 h, centrifuged at 1,200 r/min for 5 min, washed 3 times with PBS, then added with 120 µl of RNAse A (Siemo, USA) in the dark, bathed in 37°C water for 40 min, added with 500 µl of PI (Sigma, USA) for staining. After mixing, the sample was placed at 4°C for 30 min in dark. The cell cycle was determined by flow cytometry (Beckman Coulter, USA) when the red fluorescence was at an excitation wavelength of 488 nm.

After 48 h of cell transfection, the cells were digested with trypsin (Thermo, USA) without EDTA, collected in a flow tube, centrifuged at 2,000 r/min for 30 min, discarded for supernatant, then washed 3 times with pre-cooled PBS, centrifuged at 2,000 r/min for 20 min, and again discarded for supernatant. According to Annexin-V-FITC Apoptosis Detection Kit (Sigma, USA), HEPES buffer, Annexin-V-FITC, and PI (50:1:2) were combined into Annexin-V-FITC/PI dye solution, then 100 µl of which was added into the sample, and cultured at room temperature for 15 min. Thereafter, 1 ml of HEPES buffer (Thermo, USA) was added in the sample and mixed. Apoptosis was measured by flow cytometry at an excitation wavelength of 488 nm.

Statistical analyses

The data were processed using SPSS 21.0. The measurement data were expressed as mean ± standard deviation. The comparison among multiple groups was performed by one-way analysis of variance. The pairwise comparison of mean values among multiple groups was conducted by Tukey post-hoc test. A difference of $P<0.05$ was statistically significant.

Results

MiR-29a-3p negatively regulated MMP-2 gene

The biological prediction site www.targetscan.org predicted that miR-29a-3p and MMP-2 had specific binding sites (**Figure 1A**). The dual-luciferase reporter assay showed that the luciferase activity in the Wt-MMP-2 subgroup of the miR-29a-3p mimic group was lower than that in the NC mimic group ($P<0.05$). Whereas, the luciferase activity in the Mut-MMP-2 subgroup did not change prominently ($P>0.05$). It can be seen that miR-29a-3p could specifically target the negative regulation of the MMP-2 gene. See **Figure 1B**.

Expression of miR-29a-3p and MMP-2

To study how miR-29a-3p regulates the MMP-2 gene and effects on the biological characteristics of smooth muscle cells in rats with AAA, we determined the expressions of miR-29a-3p and MMP-2 mRNAs by qRT-PCR, and MMP-2 protein by Western blot. Compared with the Normal group, miR-29a-3p in the other groups was down-regulated, and MMP-2 expression was up-regulated (all $P<0.05$). Compared with the Model group, the level of miR-29a-3p was up-regulated in miR-29a-3p mimic group and miR-29a-3p mimic + oe-MMP-2 group (both $P<0.05$); the levels of MMP-2 in miR-29a-3p mimic group and si-MMP-2 group were reduced (all $P<0.05$); while there was no prominent difference in the levels of MMP-2 in NC mimic group, si-NC group, miR-29a-3p mimic+oe-MMP-2 (all $P>0.05$). Compared with miR-29a-3p mimic group, the levels of MMP-2 in miR-29a-3p mimic + oe-MMP-2 group were elevated (both $P<0.05$). See **Figure 1C-E**.
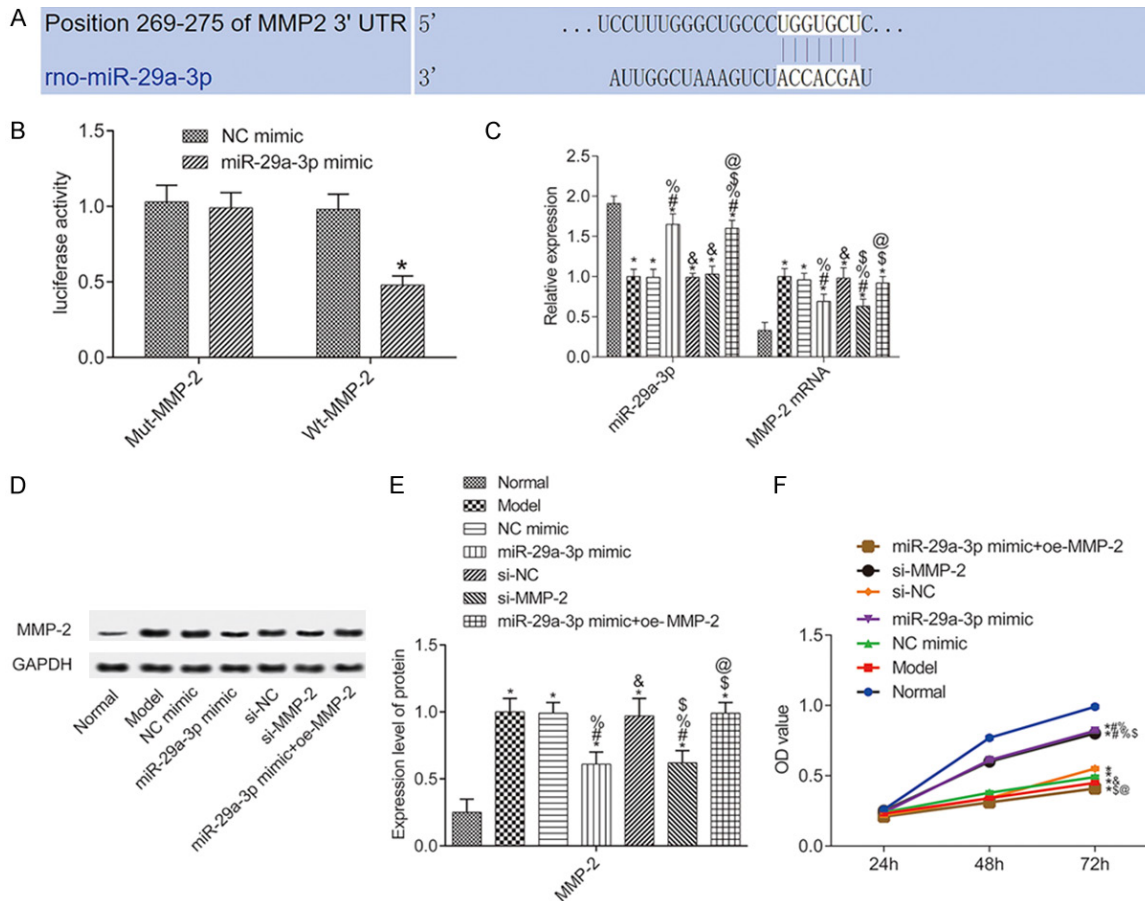
Figure 1. MiR-29a-3p targeted negative regulation of the MMP-2 gene. A. The sequence of the 3'-UTR segment of MiR-29a-3p binding to MMP-2; B. Luciferase activity determined by dual luciferase assay; C. MiR-29a-3p and MMP-2 mRNA levels in cells; D. Protein band of MMP-2; E. Protein level of MMP-2; F. Cell proliferation determined by MTT assay. *$P<0.05$ vs. Normal group; #$P<0.05$ vs. Model group; &$P<0.05$ vs. NC mimic group; $$P<0.05$ vs. MiR-29a-3p mimic group; %$P<0.05$ vs. si-NC group; @$P<0.05$ vs. si-MMP-2 group.

Cell proliferation

The cell growth in all groups increased with time. Compared with the Normal group, the proliferation rates of smooth muscle cells in other groups were reduced (all $P<0.05$). Compared with Model group, there was no prominent difference in the proliferation rate of smooth muscle cells in NC mimic group, si-NC group, and miR-29a-3p mimic + oe-MMP-2 group (all $P>0.05$), while the proliferation rate in miR-29a-3p mimic group and si-MMP-2 group was elevated (both $P<0.05$). Compared with miR-29a-3p mimic group, the proliferation rate in miR-29a-3p mimic + oe-MMP-2 group was reduced ($P<0.05$). See **Figure 1F**.

Cell cycle

The other groups had more smooth muscle cells in phase G1, and fewer in phase S than the Normal group (all $P<0.05$). Compared with the Model group, there was no statistical difference in the cells at each stage in the NC mimic group, si-NC group, miR-29a-3p mimic + oe-MMP-2 group (all $P>0.05$); while the miR-29a-3p mimic group and si-MMP-2 group had fewer cells at phase G1, and more cells at phase S (all $P<0.05$). Compared with the miR-29a-3p mimic group, miR-29a-3p mimic + oe-MMP-2 group had more cells in phase G1 and fewer cells in phase S (both $P<0.05$). See **Figure 2**.

Apoptosis determined by flow cytometry

Compared with the Normal group, the apoptosis rates of smooth muscle cells in other groups were elevated (all $P<0.05$). Compared with Model group, there was no prominent difference in the apoptosis rate of smooth muscle cells in NC mimic group, si-NC group, and miR-29a-3p mimic + oe-MMP-2 group (all $P>0.05$);
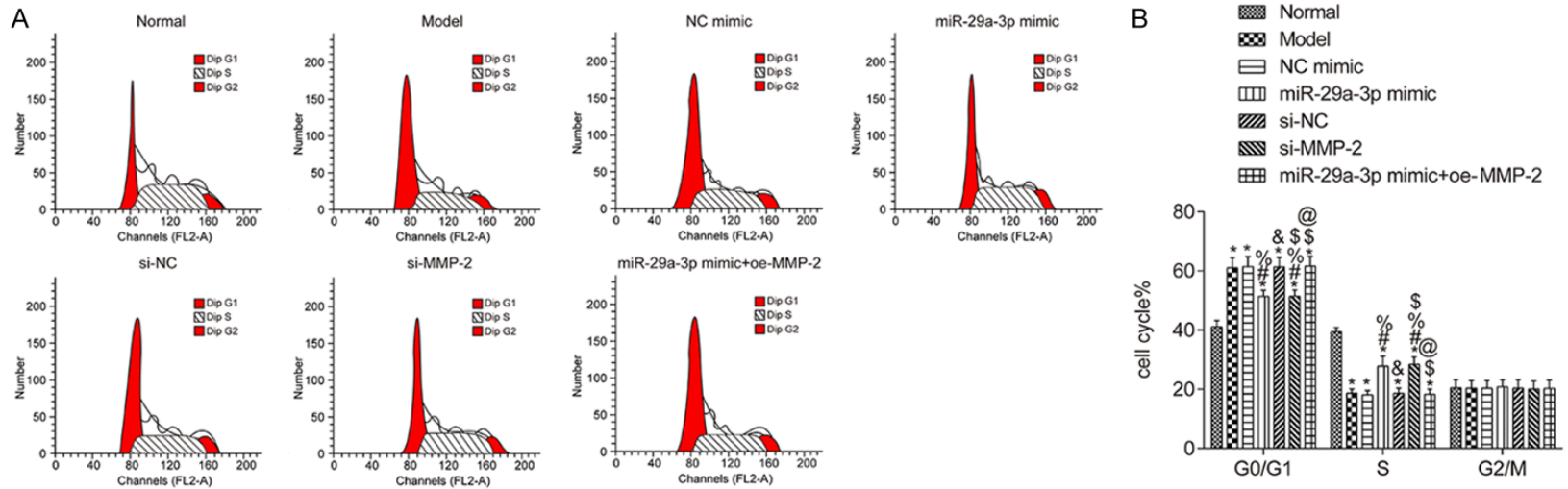
Figure 2. Cell cycle determined by flow cytometry. A. Cell cycle of each group determined by flow cytometry; B. Distribution of cell cycle in each group. *P<0.05 vs. Normal group; #P<0.05 vs. Model group; &P<0.05 vs. NC mimic group; $P<0.05 vs. MiR-29a-3p mimic group; %P<0.05 vs. si-NC group; @P<0.05 vs. si-MMP-2 group.
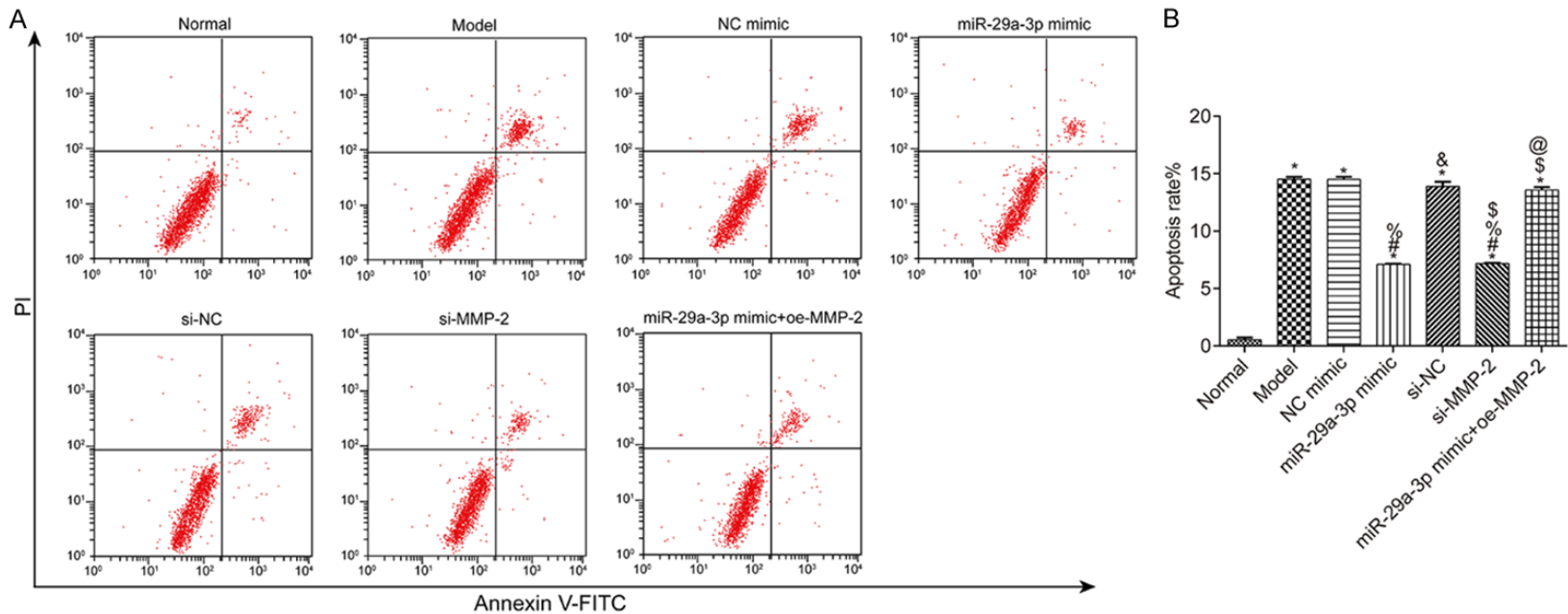
Figure 3. Apoptosis determined by flow cytometry. A. Annexin V-FITC of each group determined by flow cytometry; B. Apoptosis rate of each group. *P<0.05 vs. Normal group; #P<0.05 vs. Model group; &P<0.05 vs. NC mimic group; $P<0.05 vs. MiR-29a-3p mimic group; %P<0.05 vs. si-NC group; @P<0.05 vs. si-MMP-2 group.
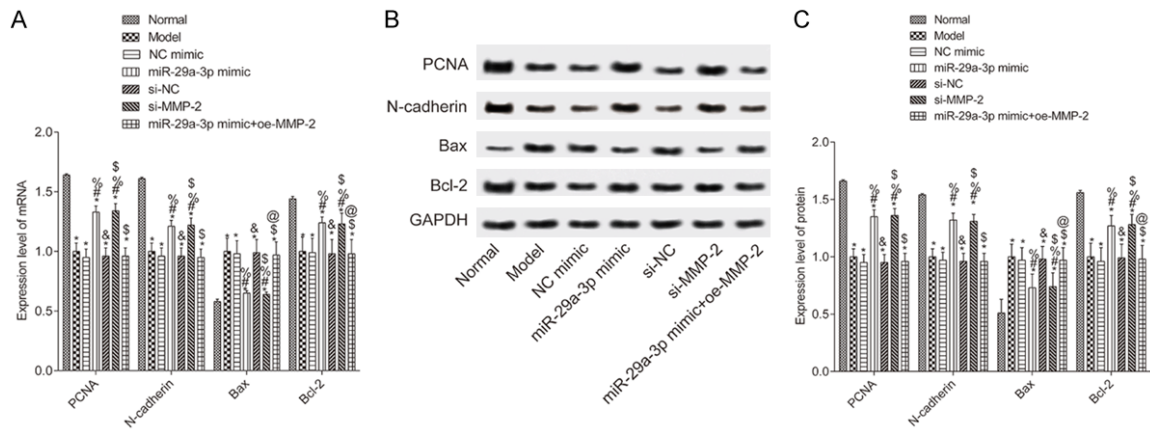
Figure 4. mRNA and protein levels of PCNA, N-cadherin, Bax and Bcl-2. A. mRNA levels of PCNA, N-cadherin, Bax, and Bcl-2 in each group; B. Protein band of PCNA, N-cadherin, Bax, and Bcl-2; C. Protein level of PCNA, N-cadherin, Bax, and Bcl-2 in each group. *P<0.05 vs. Normal group; #P<0.05 vs. Model group; &P<0.05 vs. NC mimic group; $P<0.05 vs. MiR-29a-3p mimic group; %P<0.05 vs. si-NC group; @P<0.05 vs. si-MMP-2 group.

while the apoptosis rates in miR-29a-3p mimic group and si-MMP-2 group were reduced (both P<0.05). Compared with miR-29a-3p mimic group, the apoptosis rate in miR-29a-3p mimic + oe-MMP-2 group was elevated (P<0.05). See **Figure 3**.

mRNA and protein levels of PCNA, N-cadherin, Bcl-2, and Bax

To study how miR-29a-3p regulates the MMP-2 gene and the effect on the biological characteristics of smooth muscle cells in rats with AAA, we determined the mRNA and protein expressions of proliferation-related factors PCNA, apoptosis-related factors Bcl-2, Bax and N-cadherin by qRT-PCR and Western blot. Compared with the Normal group, the other groups had reduced mRNA and protein levels of PCNA, N-cadherin, and Bcl-2 in smooth muscle cells, while elevated mRNA and protein levels of Bax (all P<0.05). Compared with the Model group, the levels were not prominently different in the NC mimic group, si-NC group, miR-29a-3p mimic + oe-MMP-2 group (all P>0.05); while the mRNA and protein levels of PCNA, N-cadherin, and Bcl-2 in miR-29a-3p mimic group and si-MMP-2 group were elevated, and the mRNA and protein levels of Bax were reduced (all P<0.05). Compared with miR-29a-3p mimic group, the mRNA and protein levels of

PCNA, N-cadherin, and Bcl-2 in miR-29a-3p mimic + oe-MMP-2 group were reduced, and the mRNA and protein levels of Bax were elevated (all P<0.05). See **Figure 4**.

Discussion

AAA is a perpetual dilatation of aortaventralis (from the diaphragm and its bifurcation to the left and right arteria iliaca communis), which presents as 50% larger than the normal ones, or a diameter of more than 3 cm [24]. Most aneurysms exist in the infrarenal aorta, near the bifurcation of aorta. Pathological processes involved in the occurrence of degenerative AAA include up-regulation of the proteolytic pathway, apoptosis, oxidative stress, inflammation, and loss of arterial wall matrix [25]. With the increase of aortic diameter, the risk of AAA rupture increases, and the mortality after rupture is high. However, the diagnosis of AAA is difficult because most aneurysms are asymptomatic before rupture [26]. A large amount of evidence showed that miRNA plays an essential role in controlling basic cell processes, including the formation of aneurysms [27]. The miRNA expression in various human tumors changes frequently, which indicates that miRNA may act as a new kind of tumor promoter or inhibitor [28].

Our results demonstrated that miR-29a-3p was a related miRNA that regulated VSMC proliferation in AAA. The function of miR-29a-3p was determined by transfecting miR-29a-3p analogs into VSMCs, which lead to an increase in VSMC proliferation and in the level of mRNA/DNA replication gene PCNA. Subsequent analysis showed that miR-29a-3p may facilitate the proliferation of VSMCs by reducing the expression of MMP-2. In addition, different physiological death signals and pathological cell damage activate the apoptosis pathway of genetic programming. Apoptosis is two main downstream pathways of cell death signals, one of which is the pathway induced by caspase and organelle dysfunction, and the other pathway is featured by the induction of mitochondrial dysfunction [29]. The activation of MMP-2 in the process of apoptosis is accompanied by the lysis of N-cadherin on the cell surface [30].

In the current study, MMP-2 was selected as the target gene of miR-29a-3p according to TargetScan. Duel-luciferase reporter assay confirmed that miR-29a-3p targeted 3'-UTR of MMP-2, and overexpression of miR-29a-3p prominently down-regulated the expression of MMP-2. The result of interfering MMP-2 expression was consistent with that of transfecting miR-29a-3p analog into VSMCs. The expression levels of PCNA, N-cadherin, and Bcl-2 were elevated, which facilitated the proliferation and inhibited the apoptosis of VSMCs. After the transfection of miR-29a-3p analog and the overexpression of MMP-2, the results were found to be reversed.

In conclusion, we explored the function of miR-29a-3p in VSMCs of rats with AAA and proved that miR-29a-3p could increase the growth and inhibit apoptosis of aortic smooth muscle cells. Therefore, miR-29a-3p can play an anti-tumor role in AAA. Further study about the role of miR-29a-3p in VSMCs from patients with AAA can give a superior understanding of the molecular mechanism of AAA development, and a broader perspective for the intervention, prevention, and treatment of AAA. However, the downstream signal axis of the mechanism of MMP-2 regulating aortic aneurysm is still not clear yet. MMP-2 may regulate the apoptosis of VSMCs through the lysis of N-cadherin.

Disclosure of conflict of interest

None.

Address correspondence to: Hongming Qi, Department of General Surgery, Zhuji Hospital Affiliated to Shaoxing University, No. 9 Jianmin Road, Shaoxing 312000, Zhejiang Province, China. Tel: +86-13587373953; Fax: +86-0575-87187700; E-mail: qihongming3h20@163.com

References

[1] Ryer EJ, Garvin RP, Schworer CM, Bernard-Eckroth KR, Tromp G, Franklin DP, Elmore JR and Kuivaniemi H. Proinflammatory role of stem cells in abdominal aortic aneurysms. J Vasc Surg 2015; 62: 1303-1311, e1304.

[2] Liang ES, Bai WW, Wang H, Zhang JN, Zhang F, Ma Y, Jiang F, Yin M, Zhang MX, Chen XM and Qin WD. PARP-1 (Poly[ADP-ribose] polymerase 1) inhibition protects from Ang II (Angiotensin II)-induced abdominal aortic aneurysm in mice. Hypertension 2018; 72: 1189-1199.

[3] Leeper NJ, Raiesdana A, Kojima Y, Kundu RK, Cheng H, Maegdefessel L, Toh R, Ahn GO, Ali ZA, Anderson DR, Miller CL, Roberts SC, Spin JM, de Almeida PE, Wu JC, Xu B, Cheng K, Quertermous M, Kundu S, Kortekaas KE, Berzin E, Downing KP, Dalman RL, Tsao PS, Schadt EE, Owens GK and Quertermous T. Loss of CDKN2B promotes p53-dependent smooth muscle cell apoptosis and aneurysm formation. Arterioscler Thromb Vasc Biol 2013; 33: e1-e10.

[4] Riches K, Angelini TG, Mudhar GS, Kaye J, Clark E, Bailey MA, Sohrabi S, Korossis S, Walker PG, Scott DJ and Porter KE. Exploring smooth muscle phenotype and function in a bioreactor model of abdominal aortic aneurysm. J Transl Med 2013; 11: 208.

[5] Salmon M, Schaheen B, Spinosa M, Montgomery W, Pope NH, Davis JP, Johnston WF, Sharma AK, Owens GK, Merchant JL, Zehner ZE, Upchurch GR Jr and Ailawadi G. ZFP148 (Zinc-Finger Protein 148) binds cooperatively with NF-1 (Neurofibromin 1) to inhibit smooth muscle marker gene expression during abdominal aortic aneurysm formation. Arterioscler Thromb Vasc Biol 2019; 39: 73-88.

[6] Emeto TI, Moxon JV, Biros E, Rush CM, Clancy P, Woodward L, Moran CS, Jose RJ, Nguyen T, Walker PJ and Golledge J. Urocortin 2 is associated with abdominal aortic aneurysm and mediates anti-proliferative effects on vascular smooth muscle cells via corticotrophin releasing factor receptor 2. Clin Sci (Lond) 2014; 126: 517-527.

[7] He Q, Tan J, Yu B, Shi W and Liang K. Long noncoding RNA HIF1A-AS1A reduces apoptosis of vascular smooth muscle cells: implications for

the pathogenesis of thoracoabdominal aorta aneurysm. Pharmazie 2015; 70: 310-315.

[8] Liu CL, Wang Y, Liao M, Wemmelund H, Ren J, Fernandes C, Zhou Y, Sukhova GK, Lindholt JS, Johnsen SP, Zhang JY, Cheng X, Huang X, Daugherty A, Levy BD, Libby P and Shi GP. Allergic lung inflammation aggravates angiotensin ii-induced abdominal aortic aneurysms in mice. Arterioscler Thromb Vasc Biol 2016; 36: 69-77.

[9] Zhai M, Guo J, Ma H, Shi W, Jou D, Yan D, Liu T, Tao J, Duan J, Wang Y, Li S, Lv J, Li C, Lin J, Zhang C and Lin L. Ursolic acid prevents angiotensin II-induced abdominal aortic aneurysm in apolipoprotein E-knockout mice. Atherosclerosis 2018; 271: 128-135.

[10] Lyon CA, Williams H, Bianco R, Simmonds SJ, Brown BA, Wadey KS, Smith FCT, Johnson JL and George SJ. Aneurysm severity is increased by combined mmp-7 deletion and N-cadherin mimetic (EC4-Fc) over-expression. Sci Rep 2017; 7: 17342.

[11] Li Y and Maegdefessel L. Non-coding RNa contribution to thoracic and abdominal aortic aneurysm disease development and progression. Front Physiol 2017; 8: 429.

[12] Zhang J, Chen H, Liu L, Sun J, Shi MA, Sukhova GK and Shi GP. Chemokine (C-C motif) receptor 2 mediates mast cell migration to abdominal aortic aneurysm lesions in mice. Cardiovasc Res 2012; 96: 543-551.

[13] Cao X, Cai Z, Liu J, Zhao Y, Wang X, Li X and Xia H. miRNA504 inhibits p53 dependent vascular smooth muscle cell apoptosis and may prevent aneurysm formation. Mol Med Rep 2017; 16: 2570-2578.

[14] Maegdefessel L, Azuma J, Toh R, Deng A, Merk DR, Raiesdana A, Leeper NJ, Raaz U, Schoelmerich AM, McConnell MV, Dalman RL, Spin JM and Tsao PS. MicroRNA-21 blocks abdominal aortic aneurysm development and nicotine-augmented expansion. Sci Transl Med 2012; 4: 122ra122.

[15] Liang B, Che J, Zhao H, Zhang Z and Shi G. MiR-195 promotes abdominal aortic aneurysm media remodeling by targeting Smad3. Cardiovasc Ther 2017; 35.

[16] Zhang Y, Liu Z, Zhou M and Liu C. MicroRNA-129-5p inhibits vascular smooth muscle cell proliferation by targeting Wnt5a. Exp Ther Med 2016; 12: 2651-2656.

[17] Su J, Lu E, Lu L and Zhang C. MiR-29a-3p suppresses cell proliferation in laryngocarcinoma by targeting prominin 1. FEBS Open Bio 2017; 7: 645-651.

[18] Wang X, Liu S, Cao L, Zhang T, Yue D, Wang L, Ping Y, He Q, Zhang C, Wang M, Chen X, Gao Q, Wang D, Zhang Z, Wang F, Yang L, Li J, Huang L, Zhang B and Zhang Y. miR-29a-3p suppress-

es cell proliferation and migration by downregulating IGF1R in hepatocellular carcinoma. Oncotarget 2017; 8: 86592-86603.

[19] Ma Y and Sun Y. miR-29a-3p inhibits growth, proliferation, and invasion of papillary thyroid carcinoma by suppressing NF-kappaB signaling via direct targeting of OTUB2. Cancer Manag Res 2019; 11: 13-23.

[20] Joviliano EE, Ribeiro MS and Tenorio EJR. MicroRNAs and current concepts on the pathogenesis of abdominal aortic aneurysm. Braz J Cardiovasc Surg 2017; 32: 215-224.

[21] Nakao T, Horie T, Baba O, Nishiga M, Nishino T, Izuhara M, Kuwabara Y, Nishi H, Usami S, Nakazeki F, Ide Y, Koyama S, Kimura M, Sowa N, Ohno S, Aoki H, Hasegawa K, Sakamoto K, Minatoya K, Kimura T and Ono K. Genetic ablation of microRNA-33 attenuates inflammation and abdominal aortic aneurysm formation via several anti-inflammatory pathways. Arterioscler Thromb Vasc Biol 2017; 37: 2161-2170.

[22] Longo GM, Xiong W, Greiner TC, Zhao Y, Fiotti N and Baxter BT. Matrix metalloproteinases 2 and 9 work in concert to produce aortic aneurysms. J Clin Invest 2002; 110: 625-632.

[23] Zhao L, Ouyang Y, Bai Y, Gong J and Liao H. miR-155-5p inhibits the viability of vascular smooth muscle cell via targeting FOS and ZIC3 to promote aneurysm formation. Eur J Pharmacol 2019; 853: 145-152.

[24] Leeper NJ, Raiesdana A, Kojima Y, Chun HJ, Azuma J, Maegdefessel L, Kundu RK, Quertermous T, Tsao PS and Spin JM. MicroRNA-26a is a novel regulator of vascular smooth muscle cell function. J Cell Physiol 2011; 226: 1035-1043.

[25] Moran CS, McCann M, Karan M, Norman P, Ketheesan N and Golledge J. Association of osteoprotegerin with human abdominal aortic aneurysm progression. Circulation 2005; 111: 3119-3125.

[26] Rizas KD, Ippagunta N and Tilson MD 3rd. Immune cells and molecular mediators in the pathogenesis of the abdominal aortic aneurysm. Cardiol Rev 2009; 17: 201-210.

[27] Parvizi M, Petersen AH, van Spreuwel-Goossens C, Kluijtmans S and Harmsen MC. Perivascular scaffolds loaded with adipose tissue-derived stromal cells attenuate development and progression of abdominal aortic aneurysm in rats. J Biomed Mater Res A 2018; 106: 2494-2506.

[28] Ni XQ, Lu WW, Zhang JS, Zhu Q, Ren JL, Yu YR, Liu XY, Wang XJ, Han M, Jing Q, Du J, Tang CS and Qi YF. Inhibition of endoplasmic reticulum stress by intermedin1-53 attenuates angiotensin II-induced abdominal aortic aneurysm in ApoE KO Mice. Endocrine 2018; 62: 90-106.

[29] Sun J, Sukhova GK, Zhang J, Chen H, Sjoberg S, Libby P, Xiang M, Wang J, Peters C, Reinheckel T and Shi GP. Cathepsin L activity is essential to elastase perfusion-induced abdominal aortic aneurysms in mice. Arterioscler Thromb Vasc Biol 2011; 31: 2500-2508.

[30] Hartland SN, Murphy F, Aucott RL, Abergel A, Zhou X, Waung J, Patel N, Bradshaw C, Collins J, Mann D, Benyon RC and Iredale JP. Active matrix metalloproteinase-2 promotes apoptosis of hepatic stellate cells via the cleavage of cellular N-cadherin. Liver Int 2009; 29: 966-978.